Lead Is Not Off Center in PbTe: The Importance of *r*-Space Phase Information in Extended X-Ray Absorption Fine Structure Spectroscopy

T. Keiber* and F. Bridges
Physics Department, University of California, Santa Cruz, California 95064, USA

B. C. Sales
Materials Science and Technology Division, Oak Ridge National Laboratory, Oak Ridge, Tennessee 37831, USA

(Received 15 May 2013; published 29 August 2013)

PbTe is a well-known thermoelectric material. Recent x-ray total scattering studies suggest that Pb moves off center along 100 in PbTe, by ~0.2 Å at 300 K, producing a split Pb-Te pair distribution. We present an extended x-ray absorption fine structure spectroscopy (EXAFS) study of PbTe (and Tl doped PbTe) to determine if Pb or Te is off center. EXAFS provides sensitive *r*- or *k*-space phase information which can differentiate between a split peak for the Pb-Te distribution (indicative of off-center Pb) and a thermally broadened peak. We find no evidence for a split peak for Pb-Te or Te-Pb. At 300 K, the vibration amplitude for Pb-Te (or Te-Pb) is large; this thermally induced disorder is indicative of weak bonds, and the large disorder is consistent with the low thermal conductivity at 300 K. We also find evidence of an anharmonic potential for the nearest Pb-Te bonds, consistent with the overall anharmonicity found for the phonon modes. This effect is modeled by a "skew" factor ($C3$) which significantly improves the fit of the Pb-Te and Te-Pb peaks for the high temperature EXAFS data; $C3$ becomes significant above approximately 150–200 K. The consequences of these results will be discussed.

DOI: 10.1103/PhysRevLett.111.095504 PACS numbers: 61.05.cj, 61.43.Dq, 72.20.Pa

Thermoelectric materials are important compounds with numerous applications ranging from solid state refrigeration to industrial heat regeneration. Good thermoelectrics are characterized by a high figure of merit $ZT = TS^2/(\rho\kappa)$, which requires simultaneously having a high Seebeck coefficient S, a low electrical resistivity ρ, and a low thermal conductivity κ, with the latter determined primarily by the lattice phonons [1]. One of the widely used materials is PbTe, which has a high ZT at elevated temperatures; ZT can be further enhanced via Tl or Na doping [2,3]. The low thermal conductivity observed in PbTe is due to a combination of properties: PbTe has soft bonds, contains heavy atoms, exhibits relatively high anharmonicity even at 300 K [4,5], and has a large Gruneisen parameter [6] and a slow speed of sound.

Although much recent work has focused on the doped materials, pure PbTe has interesting structural properties that are not yet understood. Bozin *et al.* observed a strong thermal broadening of the nearest neighbor Pb-Te (Te-Pb) peak in x-ray total scattering experiments on PbTe [7] and obtained slightly better fits if they assumed Pb was off center in the crystal along the 100 direction, leading to a split Pb-Te peak. Their off-center Pb displacement begins at approximately 100 K and increases with temperature, with a displacement of approximately 0.18 Å at 300 K. This result leads them to construct a model of local electric dipoles that emerge from the undistorted ground state upon warming [7]. However, displacements of the magnitude they suggest would significantly affect the extended x-ray absorption fine structure spectroscopy (EXAFS) data; EXAFS has the ability to resolve split peaks when the splitting $\Delta r > \pi/2k_{\max}$. Since the maximum k vector for our data is 14.4 Å^{-1}, we can resolve splittings larger than ~0.1 Å. When the splitting is small, the main effect is an increased broadening of the peak; this contribution adds in quadrature to thermal contributions [8,9]

$$\sigma^2_{\text{total}} = \frac{1}{N}\sum_i N_i[\sigma_i^2 + (r_i - r_{\text{av}})^2], \tag{1}$$

where N is the total number of bonds, N_i is the number of bonds of length r_i, and r_{av} is the average bond length.

For small splittings, it is impossible to distinguish between a thermally broadened peak with some static disorder and a slightly split peak. However, the effect of split peaks becomes noticeable beyond the resolution limit ($\pi/2k_{\max}$) and leads to interference (kinks or phase changes) in the real and imaginary parts of the *r*-space data [fast Fourier transform (FFT) of *k*-space data]. Here, we exploit this aspect of EXAFS to investigate any off-center behavior in PbTe, concentrating on the first neighbor pairs: the Pb-Te pair in the Pb L_{III}-edge data and the Te-Pb pair in the Te K-edge data.

Additionally, significant anharmonicities have been reported by Delaire *et al.* [4] in phonon mode measurements for the PbTe lattice; similar results as well as a new mode were reported by Jensen *et al.* [5]. However, the local atomic motions that lead to this anharmonicity are not yet clear. Bozin *et al.* [7] also observed an asymmetric first peak in the high T x-ray total scattering data—a sum of Pb-Te and Te-Pb correlations, but use Gaussians to fit the

data. In EXAFS, this asymmetry is described by the third cumulant $C3$ [10], and we also report this parameter for Pb-Te. However, the anharmonicities may extend beyond the nearest neighbor peak. We address this question briefly, but a full investigation is beyond the scope of this Letter.

The PbTe and PbTe:Tl samples were prepared as described in previous studies [4,11], and the preparation of the EXAFS samples is described in Refs. [11,12]. The EXAFS experiments were carried out in transmission mode at the Stanford Synchrotron Radiation Lightsource. Details are provided in the Supplemental Material [13]. Three scans were collected for each edge or temperature for averaging and to check reproducibility. The EXAFS data were reduced using standard procedures using the RSXAP package [14]; an example of the high-quality k-space data at 10 K is shown in the Supplemental Material (Fig. S1) [13] for the Pb and Te edges, to 15 and 16 Å^{-1}, respectively.

In Figs. 1(a) and 1(b), we plot the r-space EXAFS data as a function of temperature for the Pb L_{III} and Te K edges. The first peaks near 3 Å are the Pb-Te peak for the Pb L_{III} data and the Te-Pb peak for Te K-edge data. The second neighbor peaks near 4.4 Å are the Pb-Pb and Te-Te peaks in the Pb L_{III}- and Te K-edge data, respectively. Both data sets show a strong temperature dependence of all pairs, and by 300 K, the first shell is approaching the noise level. The peaks for the second neighbor pairs have an even stronger temperature dependence, with the strongest T dependence observed for the Pb-Pb peak.

To investigate the broadening of the Pb-Te pair distribution function, we have carried out detailed fits of the data to a sum of theoretical (FEFF) functions [15] for the first few shells; here, we focus on the nearest neighbor shells in the two data sets which both probe the same pair (Pb-Te and Te-Pb).

Before fitting the data, we first illustrate the difference between a split peak and a broadened peak over the short r range of the first Pb-Te peak, as shown in Fig. 2. We used the Pb-Te theoretical function generated with FEFF [15] and split the peak, with 50% shifted 0.10 Å to higher r and 50% shifted −0.10 Å to lower r. The top part shows the real part R of the Fourier transform (FT) for the original function (solid line) and also the two split functions which are partially out of phase. The lower part compares the original (unsplit) Pb-Te standard (solid line) and the two split standards added together (dotted line). Notice the significant difference in phases between the unsplit and split peaks. In general, when there is significant destructive interference, the amplitude is decreased and often there are kinks or phase shifts in $R(r)$.

Fits were carried out in r space for the Pb-Te and Te-Pb peaks; we first varied the amplitude NS_0^2, the pair distribution width σ, and the bond length r. The coordination number N is 6 for Pb-Te. S_0^2, the amplitude reduction factor from multielectron effects, is generally between 0.8 and 1.0. At low T, the lattice is well ordered and S_0^2 was determined from the average of several fits to scans at 10 K; $S_0^2 = 0.95$ for the Pb L_{III} edge and 0.92 for the

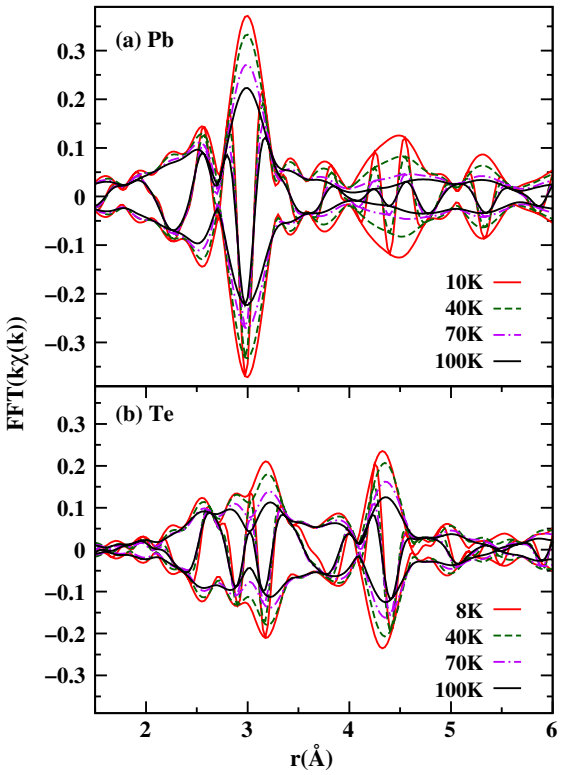

FIG. 1 (color online). r-space FFT$\{k[\chi(k)]\}$ EXAFS data for PbTe as a function of temperature. (a) Pb L_{III} edge, FT range 3.3–14.4 Å^{-1}, with a Gaussian rounding of 0.2 Å^{-1}. (b) Te K edge, FT range 3.3–15.4 Å^{-1}, with a Gaussian rounding of 0.2 Å^{-1}. In r-space data, the fast oscillating function is the real part R of the FFT, while the envelope functions are $\pm\sqrt{R^2 + I^2}$ with I the imaginary part of the FFT.

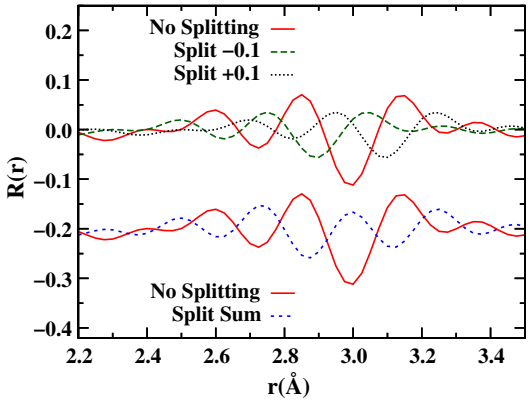

FIG. 2 (color online). The top plot shows the real part $R(r)$ of FFT$\{k[\chi(k)]\}$, generated by FEFF with no splitting (solid line). 50% of the standard was then shifted 0.10 Å to higher r, and 50% was shifted by −0.10 Å to lower r. The lower plots (shifted vertically by −0.2) compare the unsplit Pb-Te function (solid line) with the sum of the two split functions (dotted line), showing the effects of interference.

Te K edge. S_0^2 was then fixed at these values for fits as a function of temperature. The absolute value of $r_{\text{Pb-Te}}$ agrees with diffraction to within 0.01 Å [7].

To model the 100 off-center displacement proposed by Bozin *et al.* [7], we used a sum of split peaks. For this model, there is one short bond, one long bond, and four bonds approximately unshifted. These bond lengths are all specified by the off-center displacement D. Note that values of $D < 0.1$ Å are not significant because even for the long k range used, small splittings cannot be distinguished from an overall broadening. We first allowed D to vary, starting from the values in Bozin *et al.*; for these fits, $D <$ 0.1 Å for all scans and the goodness-of-fit parameter C^2 was comparable to that with no splitting. Only the values of the σ's changed, consistent with Eq. (1). To compare more directly with the results of Bozin *et al.*, we fixed the splitting $D(T)$ to the reported values (0.12 to 0.18 Å) for $150 < T < 310$ K and then allowed the other parameters to vary. In this case, C^2 increased significantly, by a factor of 4 at high temperature for the Pb L_{III}-edge data; this is an enormous decrease in the quality of the fit, and the Hamilton F test [16–18] confidence level is 0.995, that for temperatures above 200 K, a broadened peak is a much better fit than the split peak. Note that the F test uses the ratio of C^2 parameters and the number of degrees of freedom for two fits, to determine if one fit is significantly better.

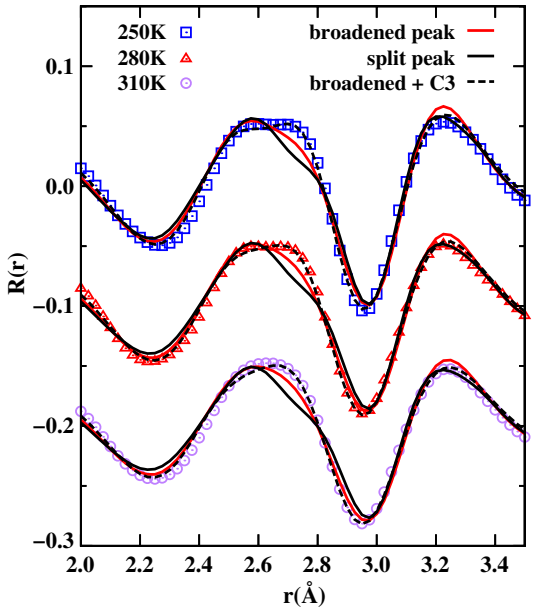

FIG. 3 (color online). Real part of FFT$\{k[\chi(k)]\}$, $R(r)$ (symbols) for the Pb data for several high temperatures. Best fit using only broadened peaks, red (gray) lines; fit using the splitting proposed by Bozin *et al.* [7], solid black line; fit including the third cumulant $C3$, dashed black lines. Using a large splitting, the fit is poor and there is a significant kink between 2.6 and 2.8 Å. The fit is significantly improved if the third cumulant $C3$ is included.

The effects of a large splitting are observed directly in plots of the real part $R(r)$ of the FFT as shown in Fig. 3 for several Pb L_{III} data sets at temperatures between 250 and 310 K. For these data, there is a significant kink from 2.6–2.8 Å in the fit using a split peak (solid black line), and the disagreement between the fits using the split peaks and fits using a broadened peak [solid red (gray) line] increases as T increases. Some fits were also carried out for 110 and 111 off-center displacements for Pb, but again C^2 increased for significant splittings D. Similar results were obtained for the Te K-edge data.

To investigate anharmonic effects [4] for the Pb-Te bond, we included the third and fourth cumulants ($C3$ and $C4$ parameters) [10] in the fits. $C3$ is a measure of the "skewness" of the pair distribution function and in k space primarily affects the phase at high k values. The $C4$ parameter determines the kurtosis, a flattening (sharpening) of the peak of the Gaussian; here, it slightly increases the amplitude at high k. However, the effect on the quality of the fit at high T is small and we do not discuss it further—see the Supplemental Material [13]. For the Pb data, which has a better signal-to-noise ratio at high k, the fit including $C3$ is significantly improved for $T \geq 190$ K, based on the Hamilton F test (confidence level >0.95); however, the smooth variation of $C3$ with T suggests that the values at lower T are probably also valid. Examples of these improved fits are also shown in Fig. 3 as dashed black lines; the dashed lines now pass through the data points.

It is also instructive to show the results in k space at high k where the effects of $C3$ are largest. In Fig. 4, we compare the original data at 280 K for the Pb L_{III} data (includes further neighbors; see the Supplemental Material [13]) with the back FFT (BFT) of the data over the r range 2.4 to 3.3 Å, plus the BFTs of the split-peak fit and the $C3$ fit (same range). The $C3$ fit follows the phase of the data very well over the entire k range; in contrast, the split peak has a large shift in phase at high k and the amplitude is too large.

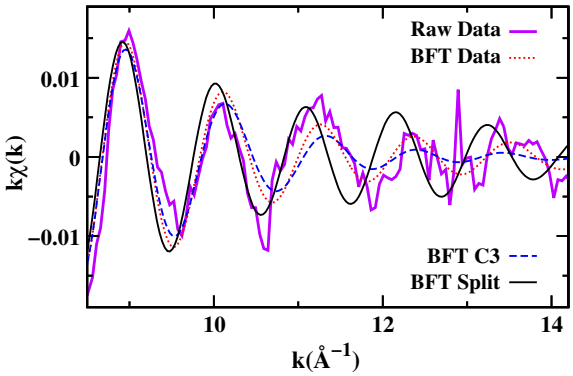

FIG. 4 (color online). $k[\chi(k)]$ for the Pb L_{III} data at 280 K compared with the BFT of the original data (dotted red line), the fit using $C3$ (dashed blue line), and using a split peak (black). The latter has too much amplitude and is out of phase above $k = 11$ Å^{-1}.

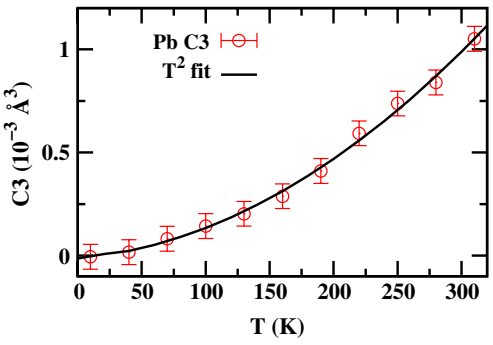

FIG. 5 (color online). The $C3$ parameter for the Pb-Te bond, from the Pb L_{III}-edge data, as a function of temperature.

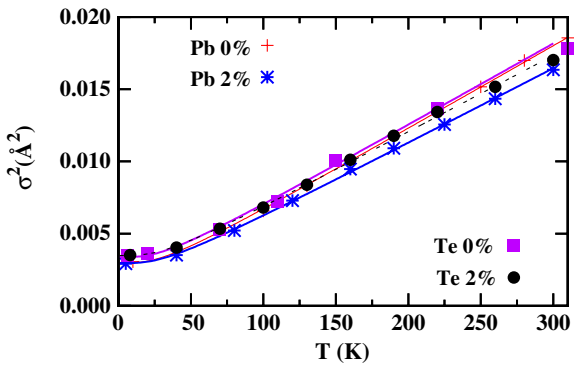

FIG. 6 (color online). $\sigma^2(T)$ for the first Pb-Te and Te-Pb pairs in PbTe. Also included for comparison are the data for PbTe doped with 2% Tl. The solid lines are fits to a correlated Debye model. The data are nearly identical; Pb-Te and Te-Pb are the same pair but probed from different atoms.

From these fits, we extracted $C3(T)$ (see Fig. 5); each point is the average value from three scans. $C3$ starts near zero at 10 K and increases quadratically [19] with T up to 310 K. Clearly, the distribution is significantly skewed at room temperature and the positive sign indicates more broadening on the high r side of the distribution, similar to the asymmetric distribution function shown at 500 K, in Bozin *et al.* [7]. Thus, starting with a broadened peak at 300 K [red (gray) line in Fig. 3], the use of a split peak model moves the fit towards the solid black line, leading to a progressively poorer fit, while increasing a $C3$ parameter moves the fit towards the dashed black line and yields a much better fit.

For each sample, we also extracted $\sigma(T)$ for the Pb-Te and Te-Pb pairs (Pb and Te edge data) from these fits as a function of temperature. In Fig. 6, we plot $\sigma^2(T)$ for pure PbTe and the 2% Tl doped sample; other samples are similar. This figure shows that the four plots of $\sigma^2(T)$ are very nearly the same. This is the expected result since the Pb-Te pair is identical to the Te-Pb pair. Also, the variation of σ^2 with T is similar but slightly smaller than the variation of U_{iso} in diffraction [7]. The static offset and correlated Debye temperatures are 0.000 61 Å^2 and 116 K for the Pb-Te pair and 0.0012 Å^2 and 120 K for the Te-Pb pair. The low values for the static offsets indicate that neither Pb nor Te atoms are off center at low T, in agreement with the low T data of Bozin *et al.* [7]. The low value of the correlated Debye temperature is consistent with PbTe having a weakly bound lattice. Einstein temperatures of similar magnitudes have been found for "rattler" atoms in other thermoelectric materials having very low thermal conductivities, such as the skutterudites [12,20] and clathrates [21,22].

Even larger effects are observed for the second neighbor peaks which decrease more rapidly with temperature than the first neighbor peaks—see Fig. 1; in addition, the Pb-Pb peak amplitude decreases approximately twice as fast as that for the Te-Te pair. This suggests substantially greater disorder of the Pb-Pb pair than for the Te-Te pair at 300 K, which may be the result of the electron lone pair on the Pb atoms producing a large distortion of the Pb-Pb distribution function. However, further analysis is needed to clarify the second neighbor distributions.

In summary, we find no evidence, up to 310 K, of a significant off-center displacement of the Pb or Te atoms from the average crystal structure position. Displacements of the magnitude proposed by Bozin *et al.* [7] would produce significant changes in the phase of the real and imaginary parts of the Fourier transform; for the Pb edge data, this displacement would introduce a large kink in $R(r)$ near 2.7 Å. We agree that thermally induced vibrations grow rapidly with T, and there is significant thermally induced disorder at 300 K, characterized by a low correlated Debye temperature, plus a growing asymmetry of the Pb-Te distribution function on the high r side of the peak. Thus, the Pb and Te atoms see an anharmonic potential as indicated by Refs. [4,5] with even larger effects for the second neighbor pairs. This may indicate that low energy shearing vibration modes are thermally activated that reduce the amplitude of the second neighbor peaks. Finally, we note a recent calculation using a maximum entropy method which suggests very large 100 off-center displacements for Pb [23] (0.25 Å at 105 K and 0.3 Å at 300 K). Such large displacements would strongly decrease the amplitude and change the shape of the Pb-Te peak and are inconsistent with our data.

EXAFS provides valuable r-space phase information for the first neighbor peak that is not available with x-ray or neutron total scattering experiments. By using this information, we can easily differentiate between a large splitting of the peak and a large asymmetric broadening. These results suggest that combinations of techniques will be important for complex systems or complex dynamics.

The EXAFS work was supported under NSF Grant No. DMR1005568. The experiments were performed at Stanford Synchrotron Radiation Lightsource, operated by the DOE, Division of Chemical Sciences. Work at Oak Ridge was supported by the U.S. Department of Energy, Basic Energy Sciences, Materials Sciences and Engineering Division.

*Corresponding author.
tkeiber@ucsc.edu

[1] B. C. Sales, in *Handbook on the Physics and Chemistry of Rare Earths*, edited by L. Eyring, K. A. Gschneidner, and G. H. Lander (Elsevier, New York, 2002), Vol. 33, Chap. 211, p. 1.
[2] J. P. Heremans, V. Jovovic, E. S. Toberer, A. Saramat, K. Kurosaki, A. Charoenphakdee, S. Yamanaka, and G. J. Snyder, Science **321**, 554 (2008).
[3] Y. Pei, A. LaLonde, S. Iwanaga, and G. J. Snyder, Energy Environ. Sci. **4**, 2085 (2011).
[4] O. Delaire, J. Ma, K. Marty, A. F. May, M. A. McGuire, M. H. Du, D. J. Singh, A. Podlesnyak, G. Ehlers, M. D. Lurnsden, and B. C. Sales, Nat. Mater. **10**, 614 (2011).
[5] K. M. O. Jensen, E. S. Bozin, C. D. Malliakas, M. B. Stone, M. D. Lumsden, M. G. Kanatzidis, S. M. Shapiro, and S. J. L. Billinge, Phys. Rev. B **86**, 085313 (2012).
[6] A. D. LaLonde, Y. Pei, H. Wang, and G. J. Snyder, Mater. Today **14**, 526 (2011).
[7] E. S. Bozin, C. D. Malliakas, P. Souvazis, T. Proffen, N. A. Spaldin, M. G. Kanatzdis, and S. J. Billinge, Science **330**, 1660 (2010).
[8] B. K. Teo, *EXAFS: Basic Principles and Data Analysis* (Springer-Verlag, New York, 1986).
[9] F. Bridges, L. Downward, J. J. Neumeier, and T. A. Tyson, Phys. Rev. B **81**, 184401 (2010).
[10] G. Bunker, Nucl. Instrum. Methods Phys. Res. **207**, 437 (1983).
[11] T. Keiber, F. Bridges, B. C. Sales, and H. Wang, Phys. Rev. B **87**, 144104 (2013).
[12] T. Keiber, F. Bridges, R. E. Baumbach, and M. B. Maple, Phys. Rev. B **86**, 174106 (2012).
[13] See Supplemental Material at http://link.aps.org/supplemental/10.1103/PhysRevLett.111.095504 for additional details about the data and calculations.
[14] C. H. Booth, "R-Space X-Ray Absorption Package, 2010," http://lise.lbl.gov/RSXAP/.
[15] A. L. Ankudinov, B. Ravel, J. J. Rehr, and S. D. Conradson, Phys. Rev. B **58**, 7565 (1998).
[16] W. C. Hamilton, Acta Crystallogr. **18**, 502 (1965).
[17] R. W. Joyner, K. J. Martin, and P. Meehan, J. Phys. C **20**, 4005 (1987).
[18] L. Downward, C. H. Booth, W. W. Lukens, and F. Bridges, AIP Conf. Proc. **882**, 129 (2007).
[19] J. M. Tranquada and R. Ingalls, Phys. Rev. B **28**, 3520 (1983).
[20] D. Cao, F. Bridges, P. Chesler, S. Bushart, E. D. Bauer, and M. B. Maple, Phys. Rev. B **70**, 094109 (2004).
[21] R. Baumbach, F. Bridges, L. Downward, D. Cao, P. Chesler, and B. Sales, Phys. Rev. B **71**, 024202 (2005).
[22] Y. Jiang, F. Bridges, M. A. Avila, T. Takabatake, J. Guzman, and G. Kurczveil, Phys. Rev. B **78**, 014111 (2008).
[23] S. Kastbjerg, N. Bindzus, M. Sndergaard, S. Johnsen, N. Lock, M. Christensen, M. Takata, M. A. Spackman, and B. B. Iversen, Adv. Funct. Mater. (in press).